Journal of Electroanalytical Chemistry 652 (2011) 18–25

Contents lists available at ScienceDirect

Journal of Electroanalytical Chemistry

journal homepage: www.elsevier.com/locate/jelechem

Synthesis and characterization of poly(propylene imine) dendrimer – Polypyrrole conducting star copolymer

Abd Almonam A. Baleg, Nazeem M. Jahed, Omotayo A. Arotiba, Stephen N. Mailu, Nicolette R. Hendricks, Priscilla G. Baker *, Emmanuel I. Iwuoha

SensorLab, Department of Chemistry, University of the Western Cape, Private Bag X17, Bellville 7535, South Africa

ARTICLE INFO

Article history:
Received 25 May 2010
Received in revised form 10 November 2010
Accepted 7 December 2010
Available online 14 December 2010

Keywords:
Star copolymer
Polypyrrole
Polypropylene imine dendrimer
Poly(propylene imine)-co-polypyrrole
Electrochemical impedance spectroscopy

ABSTRACT

A star copolymer based on poly(propylene imine) (PPI) dendrimer core (generations 1–4) and polypyrrole (PPy) shell was prepared. The synthesis procedure involved a condensation reaction between PPI surface primary amine and 2-pyrrole aldehyde to give the pyrrole-functionalized PPI dendrimer (PPI-2Py). The pyrrole units on the dendrimer backbone were polymerized chemically using ammonium persulfate as an oxidizing agent and electrochemically on a coated platinum electrode with PPI-2Py using cyclic voltammetry. The resulting star copolymer, called poly(propylene imine)-co-polypyrrole (PPI-co-PPy) was characterized using nuclear magnetic resonance spectroscopy (NMR), Fourier transform infrared spectroscopy (FT-IR), thermogravimetric analysis (TGA), scanning electron microscopy (SEM), X-ray diffraction (X-RD) and electrochemical impedance spectroscopy (EIS). NMR of PPI-2Py gave a new chemical shift at 8.1 ppm for N=CH, which confirmed the incorporation of 2-pyrrole aldehyde into the PPI dendrimer structure. Strong FT-IR bands appeared at 1634 cm^{-1} for ν(N=C) in the dendrimer moiety, and at 729 cm^{-1} for ν(C—H) at the α-position of the PPy ring. The PPI-co-PPy exhibited improved thermal stability than PPI-2Py and ionic conductivity over pristine polypyrrole as interpreted from the TGA and EIS profiles respectively. Hall effect measurements showed that the star copolymer is a semiconductor with an electronic conductivity of 0.7 S cm^{-1}.

1. Introduction

Star copolymers are branched macromolecules that have a central core to which multiple linear polymer chains are attached. Star copolymer materials are particularly useful for coatings because of their spherical structure and their ability to pack in three dimensions. The three dimensional structure with extended conjugated linear polymer chains give star copolymers properties that are better than the typical two-dimensional linear polymers. The conducting chains surprisingly, can provide sufficient intermolecular overlap to give solid materials with electrical conductivities higher than the corresponding linear, non-star conductive polymers [1].

Polypyrrole (PPy) exhibits good electrical conductivity and high air stability and is a useful conductive polymer. Polypyrrole has become a material of importance because of its wide range of technological applications in several areas such as secondary batteries [2], electrochromic display devices [3], light-emitting diodes [4], capacitors [5], sensors [6], membranes [7] and enzyme electrodes [8]. Electrical transport in polymeric materials [9] has become an area of increasing research interest because these materials have potentials for solid-state devices. However, polypyrrole and other conducting electroactive polymers are limited in practical use due to their very brittle structure and insolubility, which give rise to processing difficulties [10]. Synthesis of conducting star, graft or block copolymers are some of the effective ways to improving the processability of conducting polymers [11,12]. Graft and block copolymerization permit chemical linkage between the insulating matrix (end groups) and the conjugated polymer thus enhancing chemical stability of polymer [13].

Poly(propylene imine) (PPI) dendrimers are highly branched macromolecules terminated with amino groups with a number of interesting characteristics. They can be used as hydrogen donors because of their high density of amino groups [14]. Dendrimers, with their easily accessible multiple terminal or end functional group, are ideal for the construction of star-shaped polymers [15]. Electrochemistry and sensor application of pristine PPI, metallo-PPI and PPI-gold nanocomposites have been studied by our group [16–18]. The nanoscale structures of dendrimers have a variety of other applications in the fields of coatings, chemical sensors catalytic nanoreactors, drug delivery systems and liquid crystalline dendrimers [19].

Dendrimer-star copolymers [20] are novel types of molecular architecture, in which many linear homo- or block copolymer

* Corresponding author. Tel.: +27 21 9593051; fax: +27 21 9593055.
E-mail address: pbaker@uwc.ac.za (P.G. Baker).

1572-6657/$ - see front matter © 2010 Elsevier B.V. All rights reserved.
doi:10.1016/j.jelechem.2010.12.010

chains are attached to a dendrimer core. Dendrimer-star copolymers combine the properties of conventional polymers with those of dendrimers [21]. Two general methods have been used to prepare dendrimer-star copolymers. One is to link a monofunctional linear polymer onto the dendrimer surface [22] while the other is the growth of arm polymer chains from the surface of dendrimer by "controlled/living" polymerizations, such as anionic polymerization [23] ring-opening polymerization (ROP) [24], and atom transfer radical polymerization (ATRP) [25]. Darcos et al. [26], described the synthesis of hybrid dendrimer-star polymers via the reversible addition-fragmentation transfer (RAFT) polymerization process. Conducting star-shaped copolymers consisting of a regioregular poly(3-hexylthiophene) arm attached to a polyphenylene dendrimer core have been reported by Wang et al. [27]. The conductivity of the polyamidoamine (PAMAM) dendrimers modified with cationically substituted naphthalene diimides have also been reported by Miller et al. [28].

This work reports the synthesis and characterization of novel conducting star copolymers based on a poly(propylene imine) dendrimer core and polypyrrole shell. The synthesis was carried out in two steps. In the first step, chemical condensation reaction between the amino functional surface group of PPI dendrimer and 2-pyrrole aldehyde gave a functionalized dendrimer containing oxidizable pyrrole groups. In the second step, chemical and electrochemical oxidative copolymerization of pyrrole with the pyrrole-functionalized PPI dendrimer was carried out. The star copolymers were characterized by Fourier transform infrared spectroscopy, scanning electron microscopy (SEM), cyclic voltammetry (CV), electrochemical impedance spectra and Hall effect measurements.

To the best of our knowledge this is the first report of conducting star copolymers with a PPI-dendrimer core and PPy shell. The polymer growth occurred at the α-position coupling of PPI-2Py dendrimer end group and this constitutes the polypyrrole arms of the star copolymers. It is envisaged that the novel star copolymers will find application in biosensors as platforms for immobilizing biological elements such as enzymes, antibodies and DNA.

2. Experimental

2.1. Materials and methods

Ultra pure water with resistivity 18.2 MΩ cm^{-1} was prepared using a Millipore Synergy water purification system. poly(propylene imine) dendrimer from SyMO-Chem, Eindhoven, Netherlands was used as received. The 2-pyrrole carboxaldehyde, lithium perchlorate, ammonium persulfate, dichloromethane (DCM) and methanol of analytical grade from Sigma–Aldrich were used as received. The pyrrole (Py) monomer (Aldrich) was distilled prior to use. The IR spectra were recorded using a PerkinElmer Spectrum 100 – FT-IR Spectrometer. Fluorescence spectrometer from Horiba NanoLog™ 3-22-TRIAX, with double grating excitation and emission monochromators with a slit width of 3.2 nm was used. The PPI aqueous sample was prepared for fluorescence experiment by dissolving in water and solid sample of PPy and the star copolymer chemically prepared were pressed to use in the fluorescence experiment. The ^{1}H NMR (200 MHz) (Varian Gemini XR200 spectrometer), spectroscopy was carried out using $CDCl_3$ as the solvent with tetramethylsilane as an internal standard. The morphology of the samples was studied by a SEM Gemini LEO 1525 Model microscope. Powder particles were mounted onto an electrically grounded sample holder using a double-sided adhesive tape. The samples were coated with vapour-deposited gold layer in order to achieve a good quality of images and resolution. Themogravimetric analysis (TGA) was carried out using PerkinElmer, Model TGA-7 instrument. Electronic conductivity of PPy and PPI-co-PPy chemically prepared were measured by Ecopia-Hall effect measurements. Electrochemical impedance spectroscopy (EIS) measurements were recorded with Zahner (IM6ex Germany) instrument to quantify the ionic conductivity of electrochemically PPy and PPI-co-PPy and PPI-2Py in lithium perchlorate (pH 6), at perturbation amplitude of 10 mV within the frequency range of 100 kHz to 100 mHz. A three electrode electrochemical cell with argon de-aerated electrolyte was used for all electrochemical measurements. The working, auxiliary and reference electrodes used were platinum, platinum wire and Ag/AgCl (saturated 3M NaCl) respectively. Cyclic voltammetry (CV) measurement was performed on a BAS 100B electrochemical analyzer from Bioanalytical Systems, Inc. (West Lafayette, IN).

2.2. Synthesis of pyrrole-functionalized PPI dendrimer

The PPI-2Py synthesis was carried out by condensation reaction of PPI with 2-pyrrole aldehyde. A reaction mixture of poly(propylene imine) generation one dendrimer (1 g, 3.15 mmol) and 2-pyrrole aldehyde (1.2 g, 12.625 mmol) in 50 mL dry methanol was magnetically stirred under a positive pressure of nitrogen gas for 2 days in a 100 mL three-necked round-bottom flask. The methanol was removed by rotary evaporation and the residual oil was dissolved in 50 mL DCM (CH_2Cl_2); the organic phase was then washed with water (6 × 50 mL) to remove unreacted monomer. The DCM was removed by rotary evaporation and yielded the desired product as an orange oil. The method used above is a slight modification of that reported by Smith et al. [29] and Salmon & Jutzi [30]. The yield was 1.65 g, 75% (Scheme 1), the ^{1}H NMR analysis of PPI-2Py in ($CDCl_3$ 200 MHz, ppm): 1.36 (s, br, 4H, H-1), 1.74 (t, 8H, H-2), 2.43 (m, br, 12H, H-2&3), 3.51 (t, 8H), 6.21 (t, 8H, H-8), 6.47 (d, 4H, H-7), 6.86 (s, 4H, H-9), 8.1 (s, 4H, H-6). NMR of PPI-2Py gave a new chemical shift at 8.1 ppm for N═CH. Strong FT-IR bands appeared at 1634 cm^{-1} for ν(N═C) in the dendrimer moiety, and the absorption of out-of-plane bending ν(C—H) at the α-position of the pyrrole ring at 729 cm^{-1} was observed.

2.3. Chemical and electrochemical synthesis of poly(propylene imine)-co-polypyrrole (PPI-co-PPy)

The PPI-co-PPy polymer was synthesized by reacting PPI-2Py with pyrrole monomer using ammonium persulfate ($(NH_4)_2S_2O_8$) as an oxidant via chemical oxidative copolymerization, yielding conducting star copolymers with polypyrrole side chains (Scheme 2). Approximately 0.1 g (0.16 mmol) of PPI-2Py and 0.4 mL (5.65 mmol) Py were dissolved in 20 mL of chloroform with stirring. Approximately 0.265 g (11.62 mmol) of ammonium persulfate in 20 mL of distilled water was slowly added to the above solution. The polymerization reaction was carried out at room temperature for 1 h and then terminated by pouring methanol into the reaction flask. The resultant PPI-co-PPy powder was filtered and washed several times sequentially with distilled water, methanol and acetone, followed by filtering and drying in a vacuum oven at 45 °C for 12 h. The product yield was 0.145 g (33%). This method was adapted from literature with slight modification [31]. The same experimental procedure was used to prepare homo-polymer PPy except that no PPI-2Py was added to the reaction mixture.

2.4. Electrochemical synthesis of poly(propylene imine)-co-polypyrrole (PPI-co-PPy)

Onto the surface of a polished Pt electrode (2 mm diameter), 5 μL (5 mg mL^{-1}) of PPI-2Py was drop coated and allowed to dry under a blanket of nitrogen gas. The electrode was transferred to an electrochemical cell containing 5 mL of 0.1M aqueous lithium perchlorate

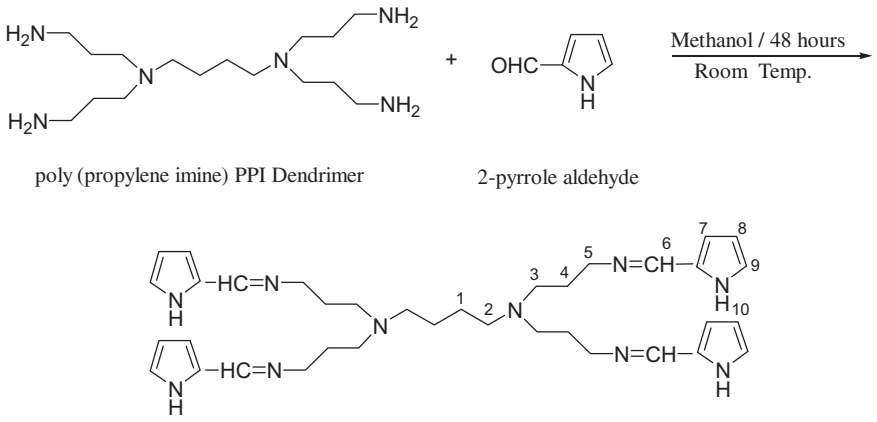

Scheme 1.

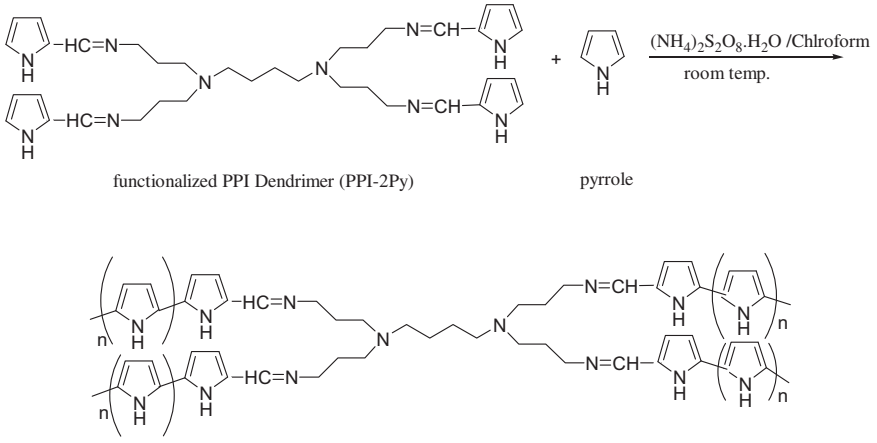

Scheme 2.

solution and 0.177 mL of 0.5M pyrrole monomer. Electrochemical polymerization was achieved by means of cyclic voltammetry (+800 mV to −650 mV) performed at a scan rate 50 mV s^{-1}, for 20 cycles. The same experimental procedure was used to prepare homo-polymer PPy onto the bare polished Pt-electrode surface (except that no PPI-2Py was coated onto the Pt-electrode surface).

3. Results and discussion

3.1. Fourier transformed infrared spectroscopy (FTIR)

The FT-IR transmission spectra of PPy, PPI-2Py and PPI-co-PPy are shown in Fig. 1. In the spectrum of PPy, the specific absorption bands appear at 3400 cm^{-1}, 1540 cm^{-1}, 1295 cm^{-1}, 1133 cm^{-1}, 1033 cm^{-1}, 890 cm^{-1}, and 777 cm^{-1}. Similar results have been reported by Depaoli and Waltaman [32] and Kang and Geckeler [33] namely, stretching vibration bands at 1543 cm^{-1} (C═C), 1295 cm^{-1} (C—C), 1130 cm^{-1} (C—N), of the pyrrole ring. The peak at 3400 cm^{-1} is assigned to the N—H stretching vibration in pyrrole. The C—H stretching and N—H bending of pyrrole can be observed at 1043 cm^{-1}, while the peak for C—H bending appears at 780 cm^{-1}. The spectrum of PPI-2Py, shows out-of-plane bending of the C—H bond located at the α-position in pyrrole ring appearing at 729 cm^{-1} [34], while the sharp band at 1634 cm^{-1} is assigned to the N═C bond stretching vibration present in the dendrimer moiety. In the PPI-co-PPy spectrum, the bands due to PPy are found at 1549 cm^{-1}, 1181 cm^{-1}, 1035 cm^{-1} and 899 cm^{-1} whereas, the sharp N═C band in PPI-2Py now appears at 1671 cm^{-1}. Furthermore, the absorbance at 729 cm^{-1} completely disappears after the polymerization, indicating that PPI-2Py was converted to PPI-co-PPy via α–α coupling of pyrrole units. The sharp band at 1043 cm^{-1} corresponds to the N—H in-plane deformation [35].

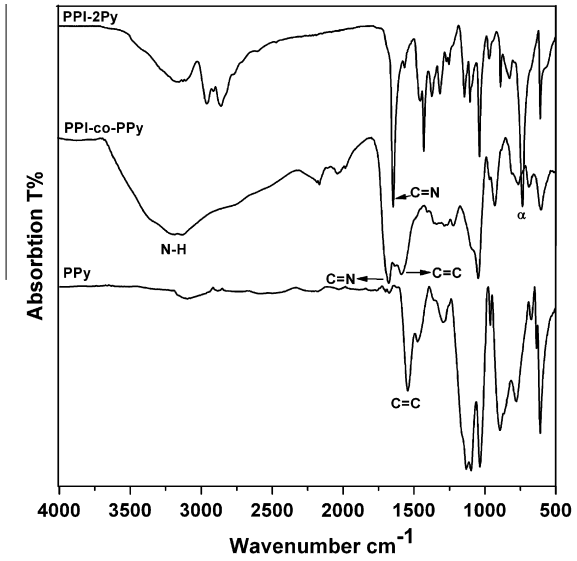

Fig. 1. FTIR spectra of pyrrole-functionalized dendrimer (PPI-2Py), star copolymer (PPI-co-PPy) and polypyrrole (PPy).

The bands at 1290 cm^{-1} and 1565 cm^{-1} are related to the (C—C) stretching vibration and (C═C) stretching mode respectively, of the pyrrole ring [36].

3.2. Fluorescence spectroscopy

The star copolymer exhibits fluorescence properties with excitation and emission bands at 385 and 422 nm respectively (Fig. 2a). In order to further validate the synthesis of a new compound, the fluorescence of the star copolymer constituents i.e. PPI and PPy were also carried out. Excitation and emission bands of 390 and 448 nm respectively were observed for PPI (Fig. 2b) and this agreed with that obtained by Wang et al. [37]. For PPy (Fig. 2c), 351 and 384 nm excitation and emission bands were observed respectively. The star copolymer was excited at the wavelengths corresponding to that of the PPI and PPy to see whether the constituent retained their individual property, but the observed emission could not be reversed to their excitation bands upon an emission–excitation scan. This shows that an entirely new compound was synthesized. In fact, the bands of the star copolymer seem to be an average of its constituents indicating the formation of a hybrid material.

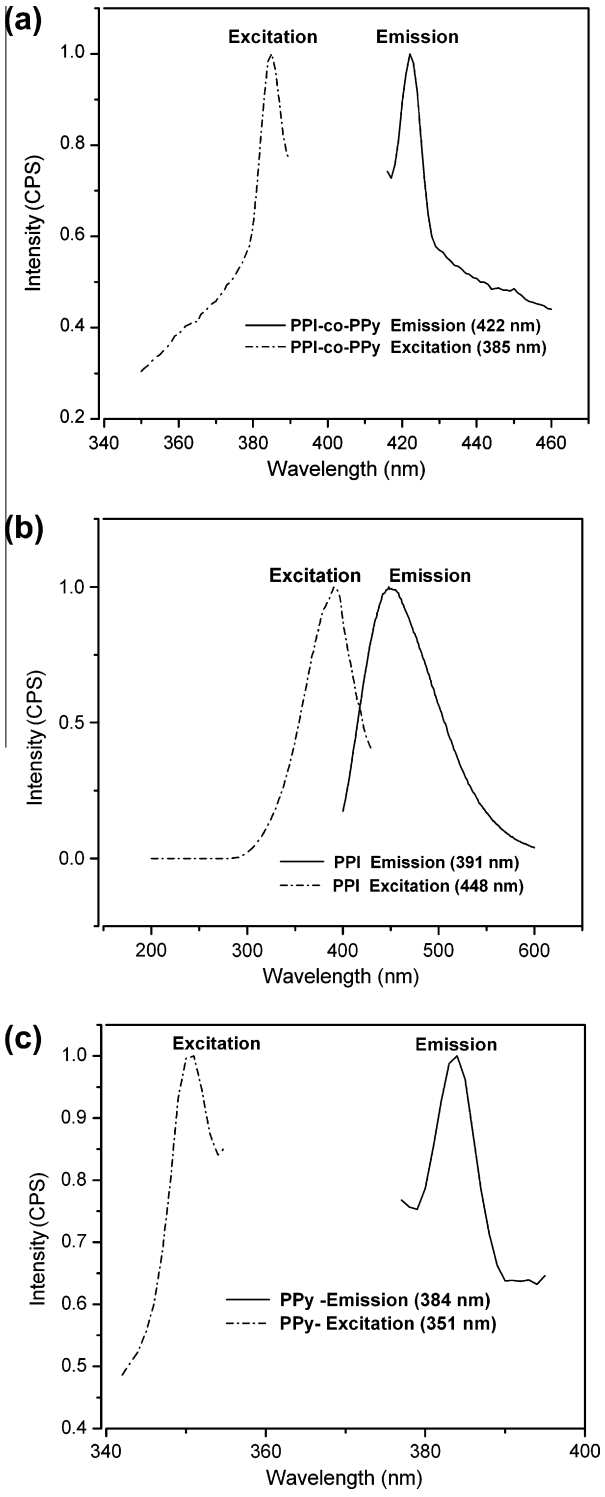

Fig. 2. Excitation and emission spectra of (A) PPI-co-PPy, (B) PPI dendrimer (C) polypyrrole.

3.3. Scanning electron microscopy (SEM)

The morphology of PPy differs depending on the method of preparation as seen in Fig. 3a and b. For chemically prepared PPy (3a), the morphology resembles densely clustered florets whereas, the electrochemically prepared PPy (3b), exhibits a dense growth of whelk-like helixes [38] initiating from the bare Pt-electrode surface with average base diameter of 1.0 μm. The morphology for the chemically prepared star copolymers resembles that of a flaky waxy material (Fig. 3d), in comparison to the orderly growth of whelk-like helixes (Fig. 3e); the surface of the PPI-2Py coated Pt-electrode surface is shown in Fig. 3c. At higher magnifications (Fig. 3f) the whelk-like helixes of the star copolymers are hollow with openings at their tapered ends and with average base diameter of 2.0 μm.

Chen et al. [38] reported the preparation of polypyrrole whelk-like helixes on the surface of a glassy carbon electrode with an average base diameter of 1.0 μm via electrochemical polymerization of pyrrole monomer in the presence of a surfactant. In addition, Chen et al. [38] have showed that high surface area and hydrophilicity of the polypyrrole whelk-like helixes enhances electrocatalytic activity as shown by the increase in oxidation current of ascorbic acid our experiments show that polypyrrole whelk-like helixes can form on a bare Pt-surface, in the absence of surfactant as well as, from a Pt-surface coated with a pyrrole-functionalized dendrimer via electro-polymerization of pyrrole in the presence of aqueous $LiClO_4$.

3.4. Electrochemical behavior of the PPI-co-PPy in PBS

Fig. 4a shows the scan rate studies (2–70 mV s^{-1}) for the PPI-co-PPy which were conducted in argon-degassed PBS (0.1M, pH 6.8). The number of electrons were calculated ($n = 2$) by using Brown-Anson equation [39]. At 50 mV s^{-1} scan rate, the surface concentration of the electroactive species was determined from the Faradaic charge (Q) passed during exhaustive electrolysis of the assembly, using same scan rate for the electrochemical polymerization. This is based on the equation $\Gamma = Q/nFA$ [40]; where n is the number of electrons transferred and F is Faraday's constant, A is the area of the electrode. The surface concentration was calculated to be 1.0271×10^{-5} mol cm^{-2}. The linear regression equations for the cathodic and anodic peaks, based on log peak current versus log v plots for diffusion kinetically – controlled scan rates were determined as: slope = 0.5127 ($r = 0.9984$) and slope = 0.5700 ($r = 0.9943$), respectively.

Fig. 4b shows the cyclic voltammetry of the electrochemical polymerization (+800 mV to −650 mV) of pyrrole on PPI-2Py modified Pt electrode performed at a scan rate of 50 mV s^{-1}, for 20 cycles. The current was observed to increase with increasing number of cycles, implying deposition of an electroactive material on the surface of the electrode. The peak at −343 mV is due to the

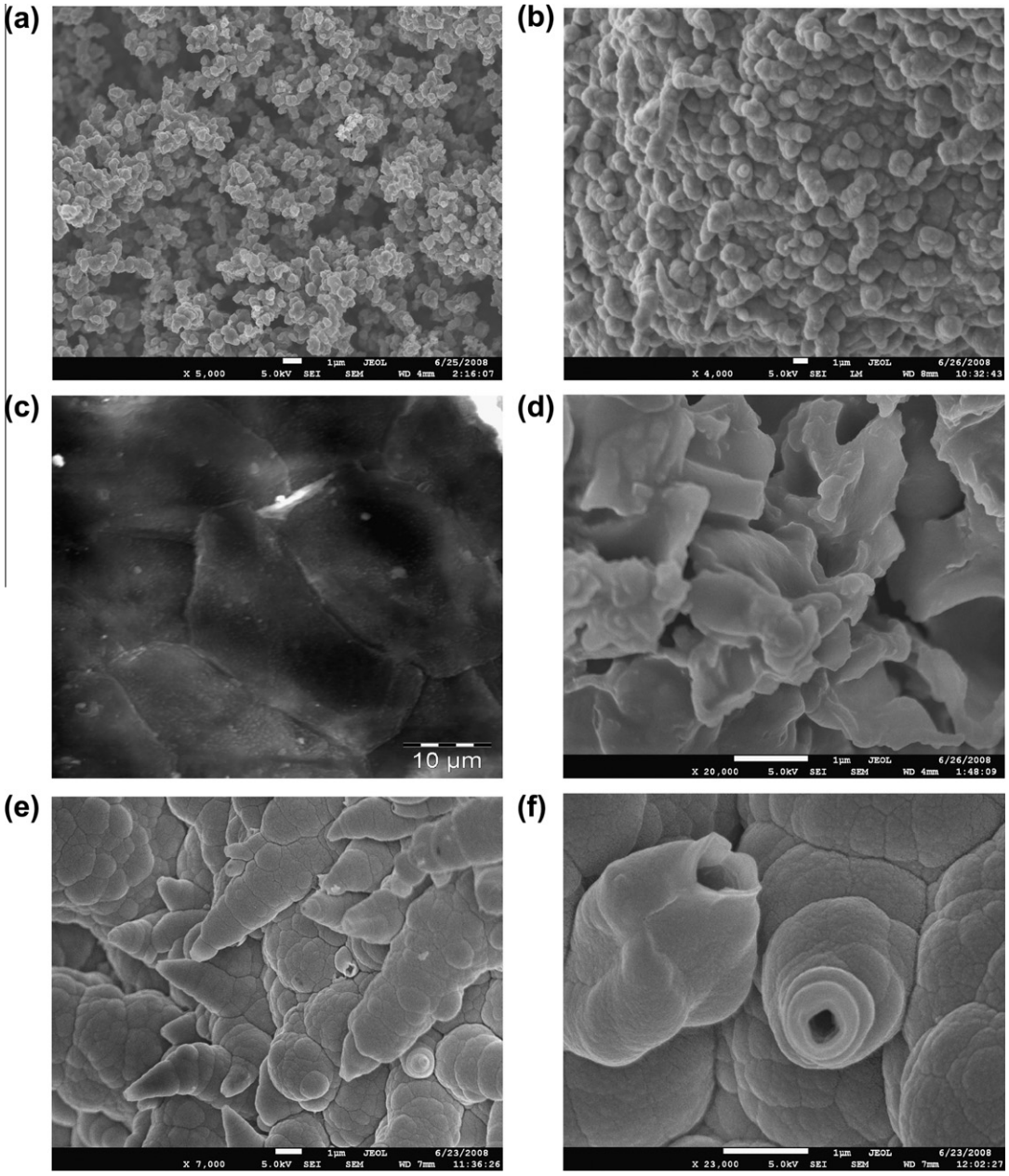

Fig. 3. SEM images of (a) Chemically synthesized PPy. (b) Electrochemically synthesized PPy on bare Pt-electrode. (c) Chemically synthesized PPI-2Py (d) Chemically synthesized. PPI-co-PPy. (e) Electrochemically polymerized PPI-co-PPy (7000×) (f) Electrochemically polymerized PPI-co-PPy (23000×).

dendrimer on the surface of the electrode and disappears after the 5th cycle. This may be due to nucleation and self-orientation of the functionalized dendrimer on the electrode surface. Although this peak disappears after the 5th cycle, the current continues to increase with increase in cycles. Growth of PPy at this step is believed to take place at the α position of the functionalized dendrimer (Scheme 2), forming the PPI-co-PPy.

3.5. Thermogravimetric analysis (TGA)

The thermograms (Fig. 5) of weight loss versus temperature for PPy, PPI-co-PPy, PPI-2Py and PPI were recoded at a heating rate of 10 °C/min in a nitrogen atmosphere. The weight change over the 50–120 °C temperature range is associated with the loss of ingress moisture present in the compounds. However, of more significance is the weight loss over the 250–700 °C temperature range due to thermal decomposition. The thermograms show a significant increase in onset temperature in the order; PPI < PPI-2Py < PPI-co-PPy < PPy with increasing pyrrole content. In addition, the residue remaining after thermal decomposition at 700 °C increases in the order PPI (0%) < PPI-2Py (38%) < PPI-co-PPy (47%) < PPy (66%). These results demonstrate that the incorporation of pyrrole onto the dendrimer increased the dendrimer thermal stability [41] and that the pyrrole content is directly proportional to the star copolymer thermal stability.

3.6. X-ray diffraction (XRD) analysis

The XRD spectra of PPy and PPI-co-PPy are presented in Fig. 6a and b, respectively. A Broadly amorphous structure of polypyrrole is observed while, the star copolymers shows additional crystalline peaks at 2θ values equal to 18.9°, 31.86°, 33.74°, 37.65°, 45.96°,

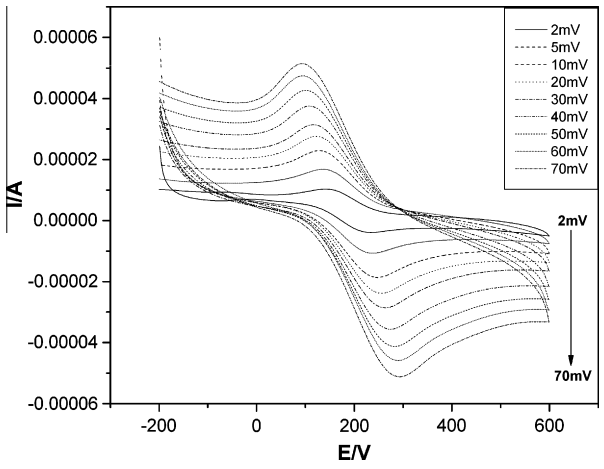

Fig. 4a. Cyclic voltammetry of PPI-co-PPy at different scan rate.

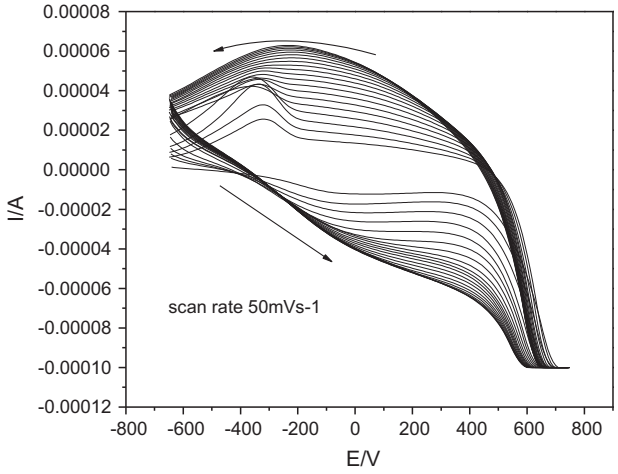

Fig. 4b. Electrochemically polymerization of Pyrrole on PPI-2Py/Pt electrode.

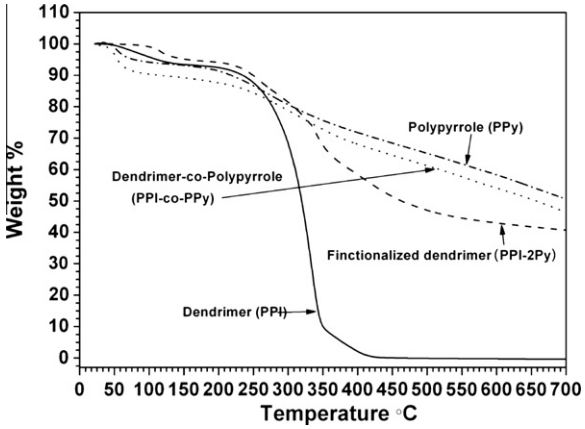

Fig. 5. Thermogravimetric analysis (TGA) for: PPy, PPI-co-PPy, PPI-2Py and PPI.

48.48° and 52.4°. However, between these crystalline peaks there are wide amorphous disordered regions within the star copolymers as is seen by the broad amorphous diffraction peak (Fig. 6a) in the $2\theta = 18–30°$ range. This broad peak is centered at 24° and corresponds to the scattering from bare polymer chains at the interplanar spacing [42]. The structure of polypyrrole does not

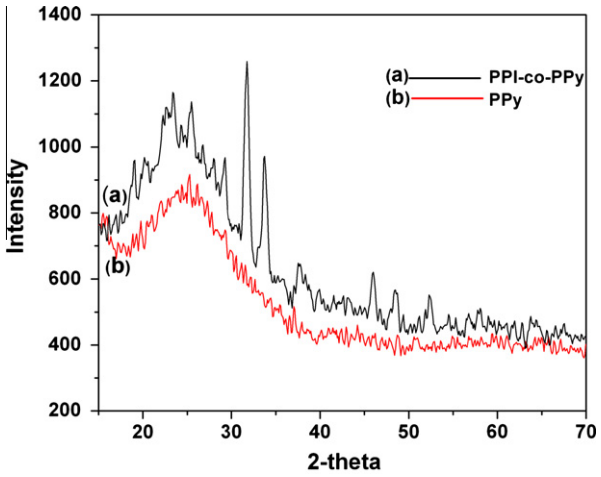

Fig. 6. XRD for (a) PPI-co-PPy and (b) PPy.

show any crystalline peaks whatsoever, hence the crystalline region observed is attributed to the dendrimer moiety in the star copolymers.

3.7. Conductivity measurements

Electronic conductivity of chemically prepared PPy and PPI-co-PPy were measured by Ecopia-Hall effect measurements. The samples was pressed into pellets (13 mm diameter) under 6 tons of pressure for 30 min at room temperature. The results showed that the PPI-co-PPy polymer is a semiconducting material, having an electronic conductivity value of 0.7 S cm^{-1} in comparison to the 1.5 S cm^{-1} of PPy. The Current–Voltage curve (Fig. 7) for PPy and PPI-co-PPy shows higher resistance at higher voltages for PPI-co-PPy when compared with PPy. This shows that PPy has higher electronic conductivity than the PPI-co-PPy polymer (conductivity is the inverse of resistance, R^{-1} = electronic conductivity). Electrical conductivity is a measure of how well a material accommodates the movement of an electric charge.

3.8. Electrochemical impedance spectroscopy (EIS)

EIS was used to estimate the ionic conductivity of PPy, PPI-2Py and PPI-co-PPy in lithium perchlorate (pH 6.1); ionic conductivity is a measure of how well a material accommodates the movement

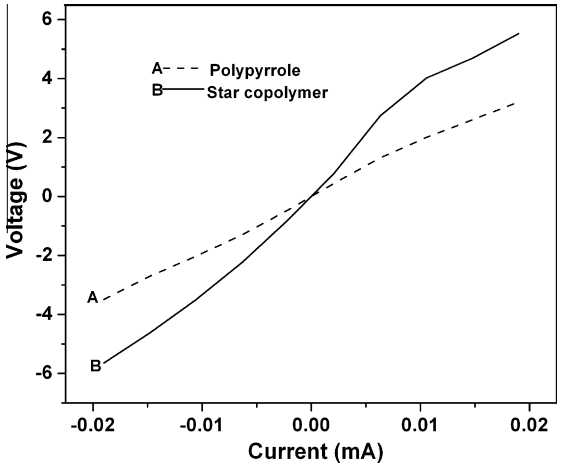

Fig. 7. IV curve for polypyrrole and star copolymers.

of ions carrying the current in the solution. The highest real impedance of 10 MΩ (not shown) was observed for PPI-2Py because the pyrrole monomer hinders the flow of ions through the dendrimer core to the platinum electrode surface. This is expected since pyrrole is only conducting in its polymer state. The marked reduction in the impedance after polymerization is an indication of the pyrrole polymerization on the dendrimer architecture. Since PPy is a conducting polymer, the PPy arm facilitates the flow of ions through the star copolymers and to the electrode surface. The Bode plot and Nyquist plots presented in Figs. 8a and 8b respectively compares the EIS of the star copolymer with the pristine PPy and bare Pt electrode. R_s models the solution resistance, R_1 and R_2 represent the resistance to the flow of the perchlorate ion through the polymer. where the constant phase element (CPE) with an α value of between 0.8 and 0.87 was used in place of capacitance for better fitting [17]. On the bare Pt electrode, lithium perchlorate showed a two time constant behavior as seen in the two ϕ_{max} of the phase angle in Fig. 8a (this can also be seen in Fig. 8b if the high frequency portion is zoomed). Since a similar two time constant is observed for the PPy and PPI-co-PPy modified electrode, it can be assumed that the impedance monitored is the charge transfer of the lithium perchlorate ions across the polymer chain. Also the relatively equal R_s value (ca 300 Ω) at a dc potential of −700 mV for all the electrodes (i.e. star copolymer, pristine polypyrrole and bare Pt-electrode surface) serves as good bases for comparing the polymers. R_{ct} is the major determining parameter which relates to the ionic conductivity and kinetic behavior which can be represented by time constant, τ. The fitting parameters using the equivalent circuit in equivalent circuit in Fig. 8a inset for the impedance plots are presented in Table 1 with fitting errors less than 5% for all the circuit elements. The phase plot at its peak maximum is characterized by frequency f_ϕ and is expressed by Eq. (1), while maximum angle ϕ_{max} is expressed by Eq. (2) [43].

$$f_\phi = \frac{1}{4\pi RC}\sqrt{1+\frac{R_{ct}}{R_s}} \tag{1}$$

$$\phi = \tan^{-1}\left(\frac{1}{1+2R_s/R_{ct}}\right) \tag{2}$$

R_{ct} and C represent charge transfer resistance (either R_1 or R_2 from Table 1) and capacitance respectively. From $\tau = R_{ct} \times C_{dl}$, Eq. (1) can be re-written as

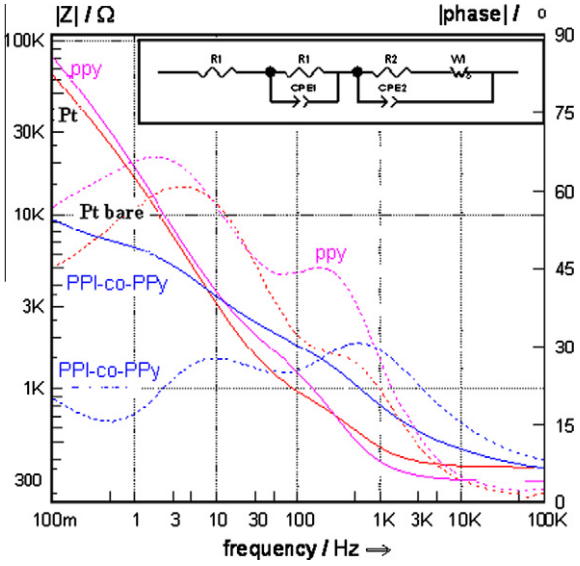

Fig. 8a. EIS Bode plots of star copolymer (PPI-co-PPy) and pristine polypyrrole (PPy) and bare Pt in 0.1 M lithium perchlorate at dc potential of -700 mV.

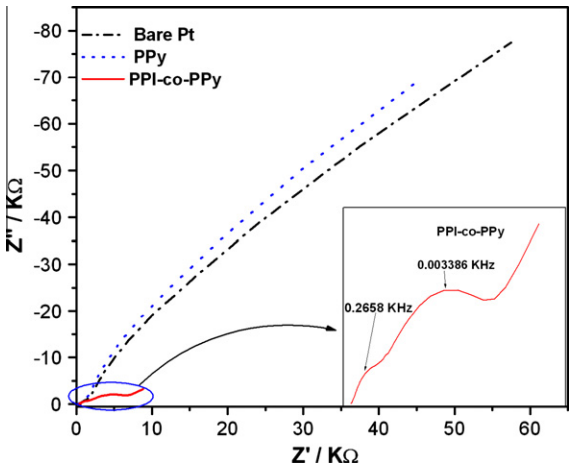

Fig. 8b. EIS Nyquist plot star copolymer, pristine polypyrrole and bare electrode in 0.1M lithium perchlorate at dc potential of -700 mV.

$$\tau = \frac{1}{4\pi f_\phi}\sqrt{1+\frac{R_{ct}}{R_s}} \quad \text{or} \quad \tau = \frac{1}{2\omega_\phi}\sqrt{1+\frac{R_{ct}}{R_s}} \tag{3}$$

(where $\omega_\phi = 2\pi f_\phi$)

These equations show that R_{ct} is inversely proportional to frequency (or τ) and directly proportional to the phase angle. From Fig. 8a, the two frequency maxima for Pt|PPI-co-PPy were higher than that of Pt|PPy while the two phase angles for Pt|PPI-co-PPy were lower than that of Pt|PPy. These observations show that the ionic conductivity of PPI-co-PPy is higher than PPy (see Table 1). This is an agreement with Eqs. (1) and (2).

The time constant, τ, is taken as a kinetic index denoting the ease of transfer of ions across the polymer membrane. This kinetic parameter was calculated from the Nyquist plot (see Table 1). Lower time constants values for both R_1 and R_2 as expected, further depicts a faster kinetics of ion transfer in PPI-co-PPy than PPy. The improved ionic conductivity of the star copolymer becomes more obvious from the Nyquist plot where it shows the least real and imaginary impedance.

A surface coverage of 99% was obtained for the star copolymer on the Pt electrode. The value was estimated from the R_{ct} value using the formula.

$$\theta = 1 - \frac{R_{ct}^{\text{modified electrode}}}{R_{ct}^{\text{bare electrode}}}$$

Kinetic parameters such as heterogeneous rate constant (k_{et}), exchange current (i_o) were also calculated from Eqs. (4)–(7) respectively.

Table 1
EIS fitted data from equivalence circuit in Fig. 8 calculated time constant.

Kinetic parameters	Pt|bare	Pt|PPI-co-PPy	Pt|PPy
R_s (Ω)	305	300	295
R_1 (kΩ)	0.360	0.217	0.632
R_2 (kΩ)	0.1431	9.404	419
CPE_1 (μF)	17.32	1.88	1.86
CPE_2 (μF)	549.4	0.306	1.7
Zw	16.79	2.7	–
$f_{\phi 1}$ (Hz)	–	662	168.5
$f_{\phi 2}$ (Hz)	–	10.03	2.24
τ_1; τ_2 (s rad^{-1})	4.76×10^{-4}; 4.7×10^{-2}	1.2×10^{-4}; 1.58×10^{-2}	9.44×10^{-4}; 7.1×10^{-2}

Table 2
Kinetics parameters of $LiCLO_4$ on PPy, Pt and PPI-co-PPy modified electrodes.

Kinetic parameters	Pt|PPI-co-PPy high freq.	Pt|PPI-co-PPy low freq.	Pt|bare high freq.	Pt|bare low freq.	Pt|PPy high freq.	Pt|PPy low freq.
ω_{max} (rad s^{-1})	8244.6	63.028	2098.2	21.28	65227.9	1058.8
τ (s rad^{-1})	1.2×10^{-4}	1.58×10^{-2}	4.76×10^{-4}	4.7×10^{-2}	9.44×10^{-4}	7.1×10^{-2}
i_0 (A)	9.868×10^{-5}	2.53×10^{-6}	7.126×10^{-5}	1.749×10^{-4}	8.637×10^{-5}	4.913×10^{-5}
k_{et} (cm s^{-1})	5.78×10^{-4}	1.48×10^{-5}	2.383×10^{-4}	2.85×10^{-4}	5.057×10^{-4}	2.876×10^{-4}

$$w_{max} = \frac{1}{R_{ct}C_{dl}} \tag{4}$$

$$\tau = R_{ct} \times C_{dl} \tag{5}$$

$$i_o = \frac{RT}{nFR_{ct}} \tag{6}$$

$$i_o = nFAK_{et}C^* \tag{7}$$

where w_{max} (frequency at the max. imaginary impedance of the semicircle) = $2\pi f$, R_{ct} = charge transfer resistance, F = Faraday constant, A = area of the electrode, C_{dl} = double layer capacitance, n = no of electron and C^* = bulk concentration of the lithium perchlorate.

The values obtained for the exchange current for the electron transfer process are given in Table 2.

The Nyquist plot Fig. 8b shows improved conductivity of the star copolymer modified electrode over bare Pt electrode and polypyrrole. Impedance spectroscopy confirms that the star copolymer has better ionic conductivity (lower R_{ct} and τ values) at −700 mV.

4. Conclusion

The novel star copolymers consisting of polypyrrole arms and a PPI-dendrimer core was successfully synthesized chemically and electrochemically. The Hall effect measurements technique showed that the star copolymers are a semiconductor having electronic conductivity of 0.7 S cm^{-1} in comparison to the 1.5 S cm^{-1} of PPy. EIS shows that the PPI-co-PPy can be a better ionic conductor at certain conditions. Owing to the holes created by the PPy arms, ions are able to flow through the star copolymer. Properties such as potential tenability, fluorescence, conductivity, biocompatible nature of the dendrimer core and interstitial voids of this material can be exploited for several sensors, membranes and photo related applications.

References

[1] F. Wang, R.D. Rauh, Reflective, Conductive Star Polymers, EIC Laboratories Inc, Norwood, MA US, 2000.
[2] A. Shimizu, K. Yamaka, M. Kohno, Bull. Chem. Soc. Jpn. 61 (1988) 4401–4406.
[3] G. Sotzing, J.R. Reynolds, P. Steel, J. Chem. Mater. 8 (1996) 882–889.
[4] D. Braun, A. Heeger, J. Appl. Phys. Lett. 58 (1991) 1982–1984.
[5] F. Larmat, J.R. Reynolds, Synth. Met. 79 (1996) 229–273.
[6] F. Selampinar et al., Synth. Met. 68 (1995) 109–116.
[7] R. Martin et al., Synth. Met. 55 (1993) 3766–3773.
[8] F. Selampinar et al., Biomaterials 64 (1997).
[9] R. Singh et al., J. Appl. Phys. 64 (1991) 2504–2508.
[10] R.Y. Qian, J.J. Qiu, D.Y. Shen, Synth. Met. 18 (1987) 13–18.
[11] M. Ak, L. Toppare, Mater. Chem. Phys. 114 (2009) 789–794.
[12] I.S. Chronakis, S. Grapenson, A. Jakob, Polymer 47 (2006) 1597–1603.
[13] S. Brahim, A. Guiseppi-Elie, Electroanalysis 17 (2005) 556–570.
[14] A.P.H.J. Schenning, E. Peeters, E.W. Meijer, J. Am. Chem. Soc. 122 (2000) 4489–4495.
[15] J. Roovers, B. Comanita, Branch. Polym. I 142 (1999) 179–228.
[16] O.A. Arotiba et al., Electrochim. Acta 53 (2007) 1689–1696.
[17] O.A. Arotiba et al., Sensors 8 (2008) 6791–6809.
[18] O.A. Arotiba et al., Chem. Today 27 (2009) 55–58.
[19] A.W. Bosman, H.M. Janssen, E.W. Meijer, Chem. Rev. 99 (1999) 1665–1688.
[20] J.L. Hedrick et al., Macromolecules 31 (1998) 8691–8705.
[21] J. Roovers et al., Macromolecules 26 (1993) 4324–4331.
[22] R.C. Hedden, B.J. Bauer, Macromolecules 36 (2003) 1829–1835.
[23] B. Comanita, B. Noren, J. Roovers, Macromolecules 32 (1999) 1069–1072.
[24] Y.L. Zhao et al., Chem. Mater. 15 (2003) 2836–3801.
[25] A. Heise et al., Macromolecules 34 (2001) 10–20.
[26] V. Darcos et al., Chem. Commun. (2004) 2110–2111.
[27] F. Wang, R.D. Rauh, T.L. Rose, J. Am. Chem. Soc. 119 (1997) 11106–11107.
[28] L.L. Miller et al., J. Am. Chem. Soc. 119 (1997) 1005–1010.
[29] G. Smith, R. Chen, S. Mapolie, J. Organometall. Chem. 673 (2003) 111–115.
[30] A. Salmon, P. Jutzi, J. Organometall. Chem. 637–639 (2001) 595–608.
[31] R. Turcu et al., Synth. Met. 119 (2001) 287–288.
[32] M.A. Depaoli, R.J. Waltaman, Polym. Sci. Polym. Chem. 23 (1985) 1687–1698.
[33] H.C. Kang, K.E. Geckeler, Polymer 41 (2000) 6931–6934.
[34] L. yan et al., Polymer 49 (1) (2007) 225–233.
[35] K.M. Cheung, D. Bloor, G.C. Stevens, Polymer 29 (1988) 1709–1717.
[36] J.W. Gardner, P.N. Bartlett, Nanotechnology 2 (1991) 19–32.
[37] D. Wang, T. Imae, M. Miki, J. Colloid Interface Sci. 306 (2,15) (2007) 222–227.
[38] G. Chen et al., Advan. Funct. Mater. 17 (2007) 1844–1848.
[39] A.J. Bard, L.R. Faulkner, Electrochemical Methods Fundamentals Applications, Second ed., Wiley, New York, 2000.
[40] J.F. Rusling, R.J. Forster, J. Colloid Interface Sci. 262 (2003) 1.
[41] L. Ningyuan, D. Shan, X. Huaiguo, Eur. Polym. J. 43 (2007) 2532–2539.
[42] J. Ouyang, Y. Li, Polymer 38 (1997) 3997–3999.
[43] M.E. Orazem, B. Tribollet, Electrochemical Impedance Spectroscopy, John Wiley & Sons, Inc, Hoboken, New Jersey, 2008. p. 315.